Research Article | Vol. 29, No. 24 / 22 Nov 2021 / Optics Express 39498
Optics EXPRESS

Non-line-of-sight optical information transmission through turbid water

ZILAN PAN,[1] YIN XIAO,[1] LINA ZHOU,[1] YONGGUI CAO,[1] MO YANG,[2] AND WEN CHEN[1,3,*]

[1]Department of Electronic and Information Engineering, The Hong Kong Polytechnic University, Hong Kong, China
[2]Department of Biomedical Engineering, The Hong Kong Polytechnic University, Hong Kong, China
[3]The Hong Kong Polytechnic University Shenzhen Research Institute, Shenzhen 518057, China
*owen.chen@polyu.edu.hk

Abstract: In this paper, a new and robust method is proposed to realize high-fidelity non-line-of-sight (NLOS) optical information transmission through turbid water around a corner. A series of 2D random amplitude-only patterns are generated by using the zero-frequency modulation method, which are used as optical information carriers. The laser beam modulated by random amplitude-only patterns propagates through turbid water, and the wave diffused by turbid water is further reflected around a corner. A single-pixel detector is used to collect light intensity at the receiving end. To demonstrate feasibility and effectiveness of the proposed NLOS free-space optical information transmission system, many optical experiments are conducted. The proposed method is fully verified by using different turbid water conditions, different separation distances around a corner and different detection angles of the single-pixel detector. Optical experimental results demonstrate that the proposed method is able to achieve high fidelity and high robustness for free-space optical information transmission through turbid water. Even when there is an obstacle behind turbid water, high-fidelity free-space optical information transmission is still realized by using the proposed method. In addition, the proposed method possesses a wide detection range at the receiving end, which is of great significance in practical applications. The proposed method is a promising application for NLOS free-space optical information transmission.

1. Introduction

Wireless data transmission plays an important role in various research areas, and has stimulated considerable interest in recent years. To satisfy the ever-increasing demands for various applications (e.g., communication [1–4]), wireless data transmission is expected to be continuously developed. There are many wireless data transmission technologies, e.g., radio-frequency [5], acoustic [6] and optical wireless [7–12]. Radio frequency transmission technology provides high-velocity waves, but it is not highly suitable for long-distance transmission since radio frequency waves attenuate rapidly (e.g., through turbid water). Acoustic transmission technology uses acoustic waves to carry information which can be restricted by low-bandwidth and noise pollution in turbid water environment. Recently, it has been found that optical wireless communication is a promising alternative for free-space data transmission through turbid water, which offers high bandwidth, low latency, and unlicensed optical spectra.

However, for free-space optical transmission through turbid water, one fundamental challenge is that turbid water has strong absorption and scattering effects on optical beams resulting from water molecules and suspended particles. In this case, it is difficult to realize high-fidelity and high-efficiency free-space optical information transmission through turbid water. Another significant challenge is to deal with the obstacles in the optical path, e.g., walls, rocks, large suspended particles and organic matters or planktonic organisms in the water, which block wave

#440002 https://doi.org/10.1364/OE.440002
Journal © 2021 Received 9 Aug 2021; revised 23 Sep 2021; accepted 24 Sep 2021; published 11 Nov 2021

Optics EXPRESS

propagation between the transmitter and the receiver. When there are obstacles in the optical path, the light dramatically attenuates. Traditional line-of-sight scheme is not suitable in this case, since a strict alignment between the transmitter and the receiver is requested. Therefore, non-line-of-sight (NLOS) optical wireless communication [13–16] has been developed, and can relieve the strict pointing and tracking requirements in line-of-sight link. In addition, it is also important to address the diffusing loss resulting from obstacles. Wavefront shaping has been developed to mitigate the attenuation problem by controlling the wavefront [17–20]. However, wavefront shaping needs feedback control using an iterative algorithm which is complicated and time-consuming. Therefore, it is highly desirable to establish a simple NLOS free-space optical information transmission system to transmit optical signals through turbid water.

In this paper, a new method is proposed to establish a high-fidelity and high-robustness laser-based NLOS transmission channel through turbid water. To the best of our knowledge, this is the first investigation of encoding signal information into 2D random amplitude-only patterns to realize high-fidelity free-space optical transmission through turbid water around a corner. In the proposed method, original signal is considered as independent pixel values, and each pixel value is encoded into a 2D random amplitude-only pattern. The generated amplitude-only patterns are sequentially embedded into spatial light modulator (SLM) to be illuminated to propagate through turbid water. The optical wave is diffused through turbid water. Subsequently, part of the diffused wave reflects from a scattering wall around the corner, and the rest of the wave is blocked. At the receiving end, a single-pixel detector [21–25] is used to record light intensity. At the receiver operation, high-fidelity signal information can be retrieved by using the collected light intensity without complicated post-processing algorithms. The proposed method is fully verified by using different turbid water conditions, different separation distances around the corner and different detection angles, and optical experimental results are quantitatively evaluated. In addition to free-space one-dimensional analog-signal transmission, it is also feasible to transmit grayscale images in the designed NLOS link through turbid water. The proposed approach can effectively overcome the challenges in conventional NLOS free-space optical data transmission methods, i.e., low-fidelity analog-signal retrieval through turbid water, low light detection, low mobility and high pointing errors.

2. Principle

Figure 1 shows a schematic experimental setup for laser-based NLOS free-space optical information transmission through turbid water around a corner. He-Ne laser with wavelength of 633.0 nm is used, and an amplitude-only spatial light modulator (SLM) serves as the transmitter. Original signal is first encoded into a series of 2D computer-generated random amplitude-only patterns which are sequentially embedded into the amplitude-only SLM.

The proposed optical encoding method is described as follows: Firstly, a 2D matrix with random real values is generated. Then, fast Fourier transform (FFT) is applied to the 2D matrix to obtain its corresponding spectrum S. Zero frequency of spectrum S is replaced by one pixel value of original signal, and a new Fourier spectrum S' is correspondingly generated. Next, inverse fast Fourier transform (IFFT) is applied to the Fourier spectrum S' to obtain an updated random amplitude-only pattern. The above steps are repeated until all the pixels of original signal are individually encoded into random amplitude-only patterns. Since the finally generated random amplitude-only pattern for each pixel value of original signal contains negative values, a positive constant w is further used to divide the generated random amplitude-only pattern (P) into two patterns ($w + P$) and (w-P) which are sequentially embedded into the SLM in optical experiments. A flow chart is further shown in Fig. 2 to illustrate the proposed optical data encoding method.

As can be seen in Fig. 1, the wave propagates in free space through turbid water which consists of skimmed milk and clean water. The diameter of skimmed milk particles ranges from 10 to 600 nm. The particles can result in strong scattering effects, including Mie scattering and

Optics EXPRESS

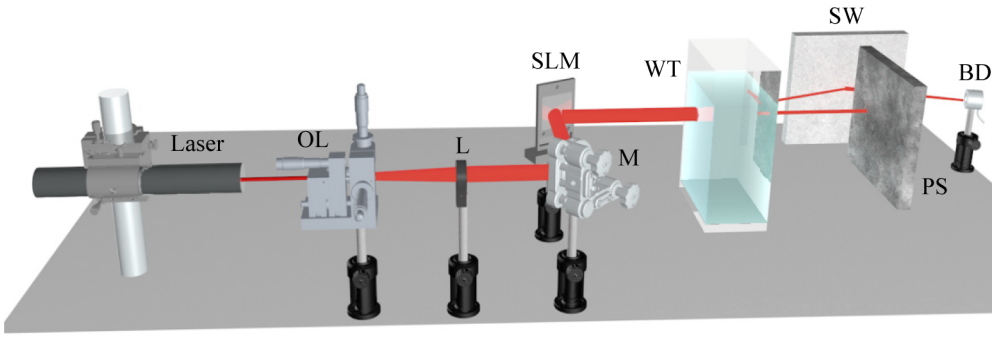

Fig. 1. Experimental setup for the proposed NLOS free-space optical information transmission system: OL: Objective lens with magnification of 40; SLM: Amplitude-only spatial light modulator; WT: Water tank; SW: Scattering wall; BD: Single-pixel (bucket) detector; L: Lens with focal length of 100.0 mm; M: Mirror; PS: Protective screen to block the beam. An ordinarily white paper is used as the scattering wall.

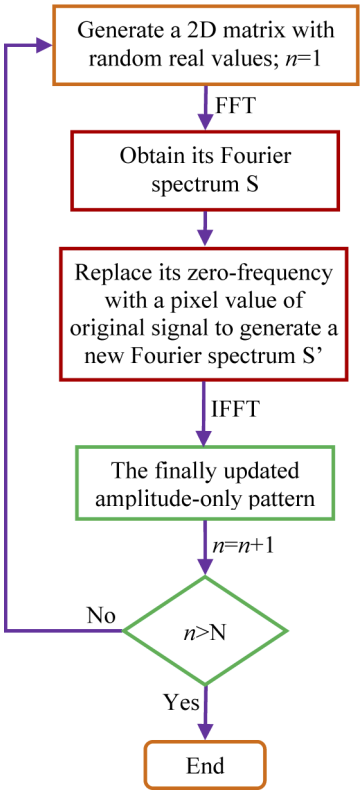

Fig. 2. Flow chart for the generation of a series of 2D random amplitude-only patterns: n denotes each pixel (1,2,3,. . .); N, the total number of pixels in original signal.

Rayleigh scattering [26]. The optical wave is attenuated rapidly by the scattering effects. In addition, when the wave propagates through turbid water, the photons encounter absorption effect. To characterize these parameters, the scattering and absorption coefficients are defined as $a(\lambda)$ and $b(\lambda)$, respectively. The total attenuation coefficient $c(\lambda)$ can be represented as the sum of

Optics EXPRESS

scattering and absorption coefficients described by

$$c(\lambda) = a(\lambda) + b(\lambda). \tag{1}$$

According to Beer-Lambert law [27], the light intensity can be calculated by

$$I(z) = I_0 e^{-c(\lambda)z}, \tag{2}$$

where I_0 denotes the incident light intensity, $I(z)$ denotes the transmitted light intensity, z denotes the path length, and $c(\lambda)$ is also called Beer's coefficient.

Behind turbid water, the diffused optical wave further propagates around a corner, as seen in Fig. 1. Part of the diffused optical wave is blocked by a protective screen as shown in Fig. 1, and other part of the diffused wave is reflected by scattering wall and then recorded by a single-pixel detector at the receiving end. The single-pixel detector is a high-sensitivity device, and is suitable for wide-range wavelength and low-light detection. Finally, the recorded light intensity is used to directly retrieve the signal. The recording and retrieval process is described by

$$\mathrm{B1} = \delta \iint [w + P(x,y)]\, e^{-2\pi j(x\xi+y\eta)} \mathrm{dxdy}|_{\xi=0,\eta=0}, \tag{3}$$

$$\mathrm{B2} = \delta \iint [w - P(x,y)]\, e^{-2\pi j(x\xi+y\eta)} \mathrm{dxdy}|_{\xi=0,\eta=0}, \tag{4}$$

$$\mathrm{B} = \mathrm{B1} - \mathrm{B2}, \tag{5}$$

where $j = \sqrt{-1}$, $(x,\ y)$ denotes the coordinate in spatial domain, (ξ, η) denotes the coordinate in frequency domain, $w + P(x,y)$ and w-$P(x,y)$ denote 2D random patterns (512×512 pixels), B1 and B2 denote the recorded intensity values, B denotes the retrieved signal, and δ denotes a scaling factor. In the proposed method, scaling factors exist between the retrieved data and original data, as shown in Eqs. (3) and (4). In the proposed method, each pixel value of original signal has been encoded into two random amplitude-only patterns, and a subtraction operation between the two corresponding intensity points recorded by single-pixel detector can be directly used for retrieving each pixel value of original signal.

3. Experimental results and discussion

A series of optical experiments are carried out to illustrate feasibility and effectiveness of the proposed NLOS free-space optical information transmission through turbid water around a corner. In Fig. 1, He-Ne laser with 17.0 mW and wavelength of 633.0 nm is used. A beam expander with a magnification of 40 is used to adjust size of the laser beam followed by the collimation using a converging lens with focal length of 100.0 mm. The collimated laser beam is reflected by a mirror and illuminates the surface of an amplitude-only SLM (Holoeye, LC-R720) with pixel size of 20.0 µm. In this study, a modulation rate of 1.25 Hz is used to conduct a proof-of-principle experiment and verify the proposed method. The angle between the incident beam and the reflected beam on the SLM is 45°. The water tank in Fig. 1 is made from PMMA, and has a dimension of 60 mm (L) × 110 mm (W) × 300 mm (H). In this study, axial distance between the SLM and water tank is 100 mm, and axial distance between water tank and scattering wall is 50 mm. Axial distance between the scattering wall and single-pixel detector is 100 mm. A single-pixel detector (Newport, 918D-UV-OD3R) and a power meter (Newport, 1936-R) are used to record light intensity at the receiving end. The active area of single-pixel detector is 1.0 cm^2. Temperature in the laboratory is set as 24°C for optical experiments.

Optics EXPRESS

3.1. Turbidity of water

The optical wave dramatically attenuates, when it propagates through turbid water. Scattering is a form of accumulation, which means that the bigger the turbidity is, the heavier its impact on quality of the retrieved signal. The effect of different turbidities of turbid water on the accuracy of the proposed free-space optical signal transmission is experimentally tested here. In the optical experimental setup shown in Fig. 1, 850 mL clean water is first prepared and placed into the water tank, and then skimmed milk in which molecules have diameters ranging from 10 to 600 nm is used to emulate turbidity. When particles have a size of 10 nm, they can lead to the forward and backward scattering effect. Therefore, skimmed milk is an optimal option to emulate all kinds of scattering effects in seawater conditions. Then, skimmed milk is added to the water tank in order to increase the turbidity. The volume of skimmed milk starts from 20 mL with an increase of 5 mL each time, and this process is repeated for five times. Three significantly different analog signals are randomly selected and tested in each milk concentration case. The wave propagation distance through turbid water is 60 mm, and separation distance around the corner, i.e., between scattering wall and protective screen, is set as 45 mm. In addition, the power just before water tank is 0.93 mW in optical experiments. To quantify turbidity level of the scattering medium, an optical power meter can be utilized to record the light intensity after propagating through the turbid water. In Eq. (2), Beer's coefficient $c(\lambda)$ can be calculated based on the light intensity before water tank, the light intensities after water tank and the propagation distance through turbid water. Beer's coefficient $c(\lambda)$ can be calculated using Eq. (2) and is employed to represent the turbidity level [28,29].

To quantitatively evaluate performance of the proposed method, signal-to-noise ratio (SNR) is calculated and defined by

$$\mathrm{SNR} = 10 \times \log_{10}\left[\frac{\sum S_{ori}^2}{\sum (S_{ori} - S_{re})^2}\right], \tag{6}$$

where S_{ori} denotes original signal and S_{re} denotes the retrieved signal. Quantitative results about the SNR variation with different concentrations of skimmed milk are shown in Fig. 3. The typically retrieved signals are shown in Figs. 4(a)–4(f), when different concentrations of skimmed milk are added to the water tank. It can be seen in Fig. 3 that the SNR values decline with the incremental of skimmed milk concentration. When the volume of skimmed milk is increased to be 40 mL, SNR values for the three retrieved analog signals are close to 20 dB. The signals retrieved at the receiving end are shown in Figs. 4(e) and 4(f), when 40 mL and 45 mL skimmed milk is respectively used. When the concentrations of skimmed milk are smaller than 40 mL, the retrieved signals have high SNR values as shown in Fig. 3 and nearly overlap with original signals as shown in Figs. 4(a)–4(d). Due to the accumulation feature of scattering, scattering becomes stronger as the skimmed milk concentration increases, which will have the heavier influence on the quality of retrieved signals. It is also illustrated in Figs. 3 and 4 that there is a steady decrease in the SNR values and light power when skimmed milk concentration is increased, and quality of the retrieved signals has a relationship with the light power. From the optical powers given in Fig. 3, it can be further observed that water turbidity significantly affects the propagating light wave, and lead to high scattering and high absorption in the free-space optical transmission channel. In addition, the optical experimental results in Figs. 3 and 4 demonstrate that the proposed method is able to directly retrieve high-fidelity and high-SNR analog signals in free-space optical transmission through turbid water around a corner.

Optics EXPRESS

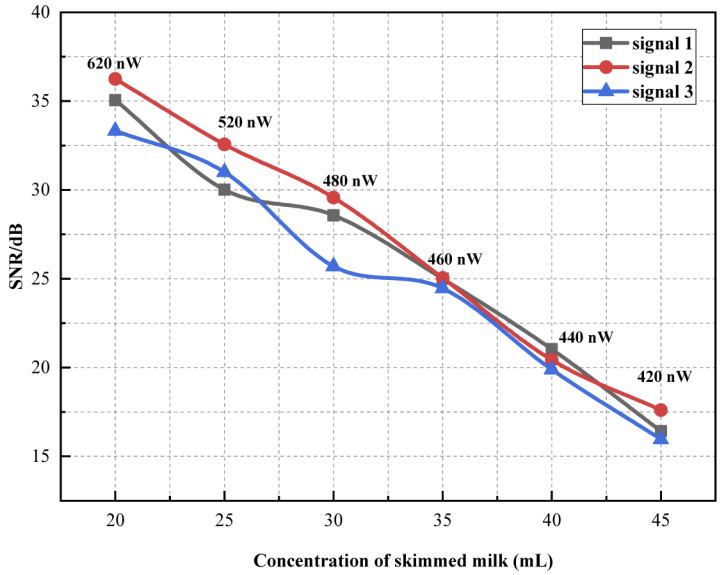

Fig. 3. A relationship between the concentration of skimmed milk and the quality of retrieved signals at the receiving end. Turbid water in the water tank consists of 850 mL clean water and different volumes of skimmed milk.

3.2. Separation distances around the corner

In addition to water turbidity, the separation distance d around the corner (i.e., between scattering wall and protective screen) in Fig. 5 can also affect optical power detected at the receiving end. In the optical experiment, a protective screen is placed between the transmitter and the receiver to block the wave, and the scattering wall is used to further reflect the diffused wave after turbid water. In optical experiments, the scattering wall is opaque. In Fig. 5, an ordinarily white paper is used to emulate the scattering wall. In this optical experiment, 850 mL clean water is mixed with 20 mL skimmed milk to be placed into the water tank. The separation distance d has an impact on the optical power detected at the receiving end, and a relationship between the separation distance d and optical power detected at the receiving end is studied here. In this case, the loss is calculated by [30,31]

$$PL = 10 \times \log_{10}\left(\frac{P_t}{P_r}\right), \tag{7}$$

where PL denotes the loss (dB), P_t denotes the power just before water tank, and P_r denotes optical power just before single-pixel detector. The power P_t just before water tank is 1.5 mW in the optical experiments. Optical experimental results are shown in Figs. 6(a)–6(d) and 7.

It can be seen in Figs. 6 and 7 that when the separation distance d increases, optical power detected at the receiving end increases and power loss decreases. In addition, accuracy of the retrieved analog signals is enhanced. These optical experimental results illustrate the high-robustness feature of the proposed NLOS free-space optical transmission method through turbid water around a corner. There is a sharply downward trend in the detected power when the separation distance is lower than 3 mm, since only a small part of optical wave is reflected by the scattering wall and others are blocked by the protective screen. When the separation distance d is lower than 3 mm, MSE values are larger than 3.55×10^{-3} and SNR values are smaller than 21.04 dB. Therefore, it can be seen in Figs. 6 and 7 that when the separation distance d is not smaller than 5 mm, the retrieved signals are always of high fidelity.

Optics EXPRESS

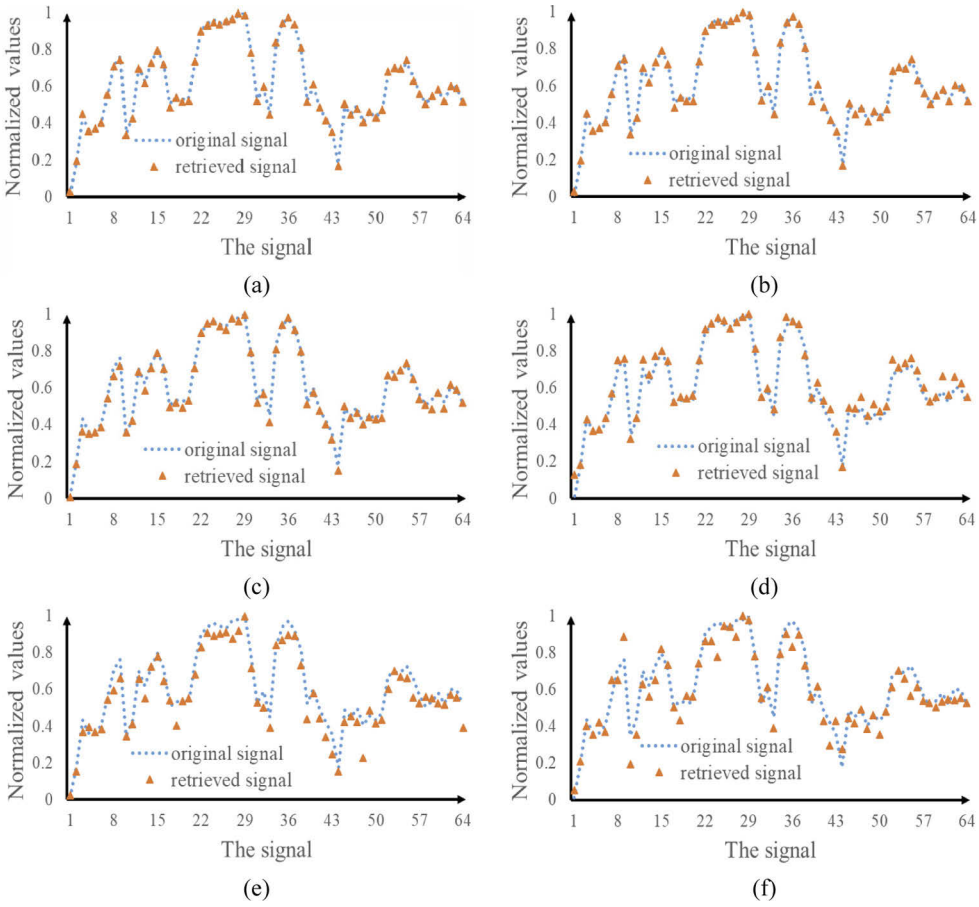

Fig. 4. (a)-(f) Comparisons between original signal and the experimentally retrieved signals at the receiving end when different concentrations of skimmed milk (i.e., 20 mL, 25 mL, 30 mL, 35 mL, 40 mL and 45 mL) are respectively used in the water tank. The signal 2 in Fig. 3 is used and typically presented here.

3.3. Detection range of the single-pixel detector

In conventional free-space optical transmission systems through complex media, the acquisition, tracking and pointing can be difficult, and pointing errors cannot be effectively mitigated. In addition, the alignment process is complicated when there are turbid water and obstacles in the wave propagation path. In the proposed NLOS free-space optical transmission system, there is no need to accurately place the single-pixel detector at the receiving end, and pointing errors can be fully suppressed.

In Fig. 8, the optical wave propagates through turbid water, and then the diffused wave is further reflected by the scattering wall. The reflected wave is detected by using a single-pixel detector placed at an arbitrary position (θ). Here, the detection angle (θ) range of single-pixel detector is further studied. In optical experiments, 850 mL clean water is mixed with 20 mL skimmed milk, and an ordinarily white paper is used as the scattering wall. The power loss is calculated to investigate performance of the developed NLOS free-space optical transmission system. It can be seen in Figs. 9 and 10 that when the single-pixel detector is arbitrarily moved and placed in a detection angle ranging from -45° to 45°, the proposed method can always realize high-fidelity free-space optical data transmission. In other words, the proposed method can

Optics EXPRESS

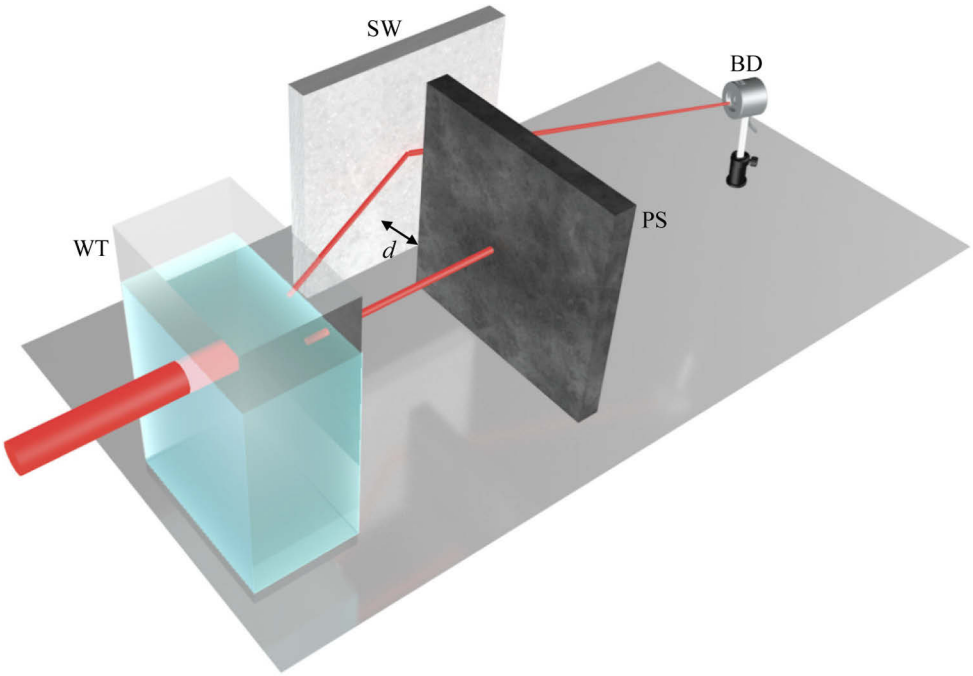

Fig. 5. A schematic optical experimental setup for wave propagation around a corner behind turbid water: d: separation distance.

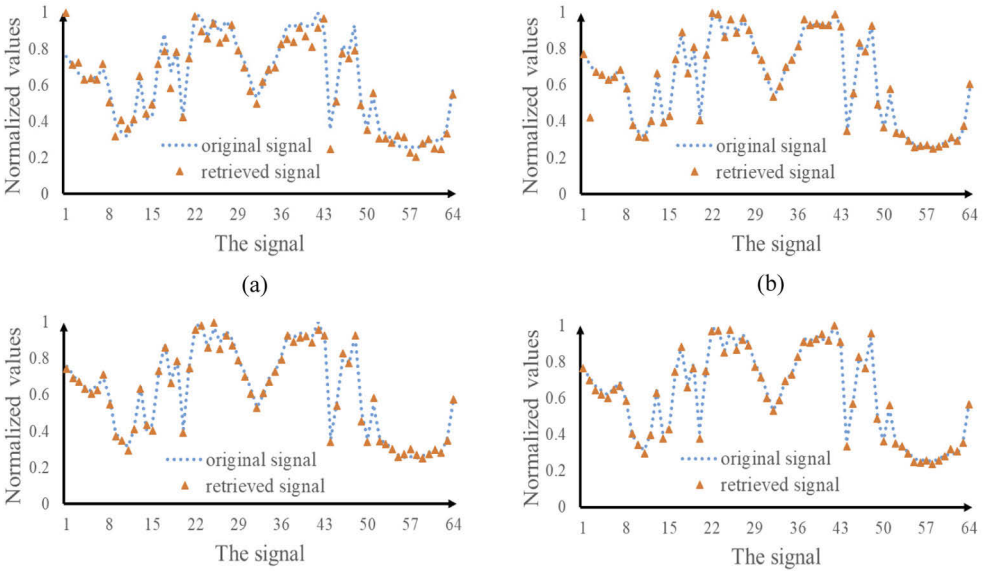

Fig. 6. (a)-(d) Comparisons between the retrieved analog signals at the receiving end in optical experiments and original signal when different separation distances are used around the corner, i.e., $d = 3$, 5, 15 and 30 mm. SNR values of the retrieved analog signals in (a)-(d) are 21.04 dB, 24.78 dB, 31.75 dB and 33.44 dB, respectively. MSE values of the retrieved analog signals in (a)-(d) are 3.55×10^{-3}, 1.50×10^{-3}, 3.01×10^{-4} and 2.04×10^{-4}, respectively.

Optics EXPRESS

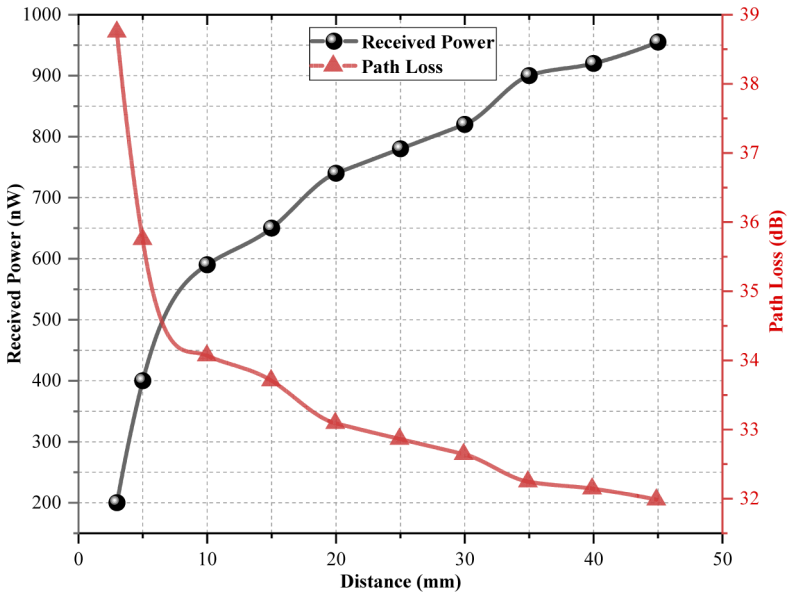

Fig. 7. The detected optical power and the loss when optical wave propagates through turbid water (850 mL clean water with 20 mL skimmed milk) and further propagates around a corner respectively with the separation distance d of 3, 5, 10, 15, 20, 25, 30, 35, 40 and 45 mm.

realize a large angular coverage at the receiving end, and high mobility is achieved. Optical experimental results demonstrate that the proposed method is robust, and pointing errors existing in conventional methods are effectively suppressed. The single-pixel detector is a high-sensitivity device, and can be applied in low-light detection environments. The proposed method can realize a multi-point connection, and can mitigate the workload of multiple carriers on each sensor.

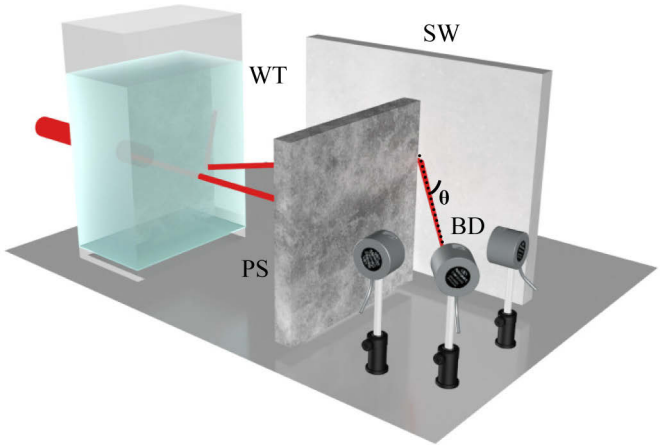

Fig. 8. A schematic setup for testing the detection range of single-pixel detector: normal direction denotes zero degree as indicated by the dotted line. θ denotes different positions of single-pixel detector. Clockwise direction denotes positive degree, and counterclockwise direction denotes negative degree.

Optics EXPRESS

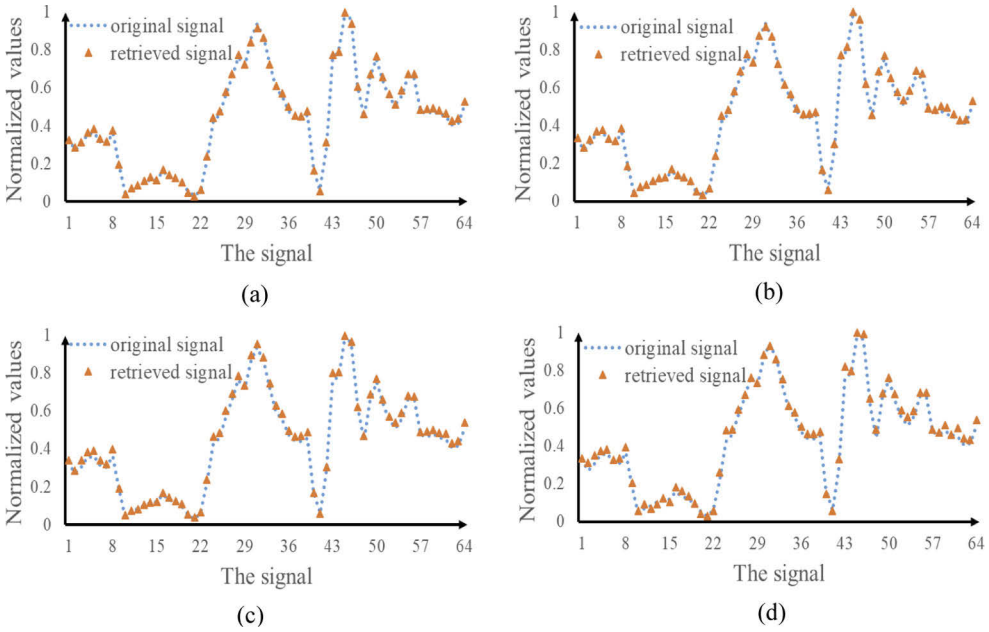

Fig. 9. (a-d) Comparisons between analog signals retrieved at the receiving end in optical experiments and the original signal when different detection angles θ={0°, 15°, 35°, 45°} of single-pixel detector at the receiving end are respectively used.

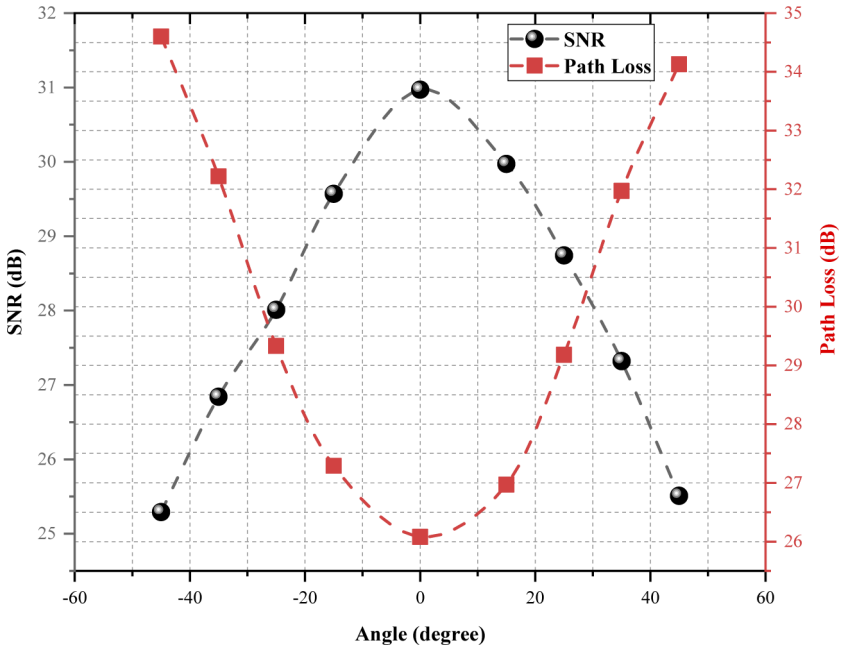

Fig. 10. SNR values of the retrieved signals and power loss obtained when different detection angles θ of -45°, -35°, -25°, -15°, 0°, 15°, 25°, 35° and 45° are respectively used.

Optics EXPRESS

3.4. Two-dimensional grayscale-image transmission

In addition to one-dimensional analog signals, the proposed method is also feasible to transmit grayscale images. In optical experiments, the turbid water consists of 850 mL clean water and 25 mL skimmed milk. In this case, the separation distance d around the corner is 25 mm, and the detection angle of single-pixel detector is set as 0°.

To quantitatively evaluate quality of the retrieved images at the receiving end, two evaluation parameters, i.e., peak signal-to-noise ratio (PSNR) [32–34] and structural similarity index measure (SSIM) [32], are calculated. The maximum SSIM value is 1, and the calculated SSIM value shows the similarity between original image and the retrieved image obtained at the receiving end.

In optical experiments, the typically retrieved images are shown in Figs. 11(a)–11(c). It can be seen in Figs. 11(a)–11(c) that the three retrieved images are of high fidelity, and PSNR values are 40.53 dB, 37.13 dB and 41.90 dB, respectively. The SSIM values for Figs. 11(a)–11(c) are 0.9929, 0.9893, and 0.9920, respectively. To clearly show the quality of retrieved images, the pixel values along the 55th row in Fig. 11(c) are shown in Fig. 12(a), and the experimentally retrieved data overlap with original data. It is also found that scaling factor between the retrieved image and original image can be further calculated to evaluate the quality. As can be in Fig. 12(b), the scaling factors are within a small range. It is illustrated that high-fidelity grayscale image can be retrieved in the proposed NLOS free-space optical data transmission method.

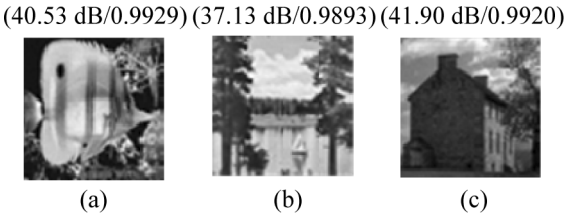

Fig. 11. Optical experimental results obtained by using single-pixel bucket detector: (a)-(c) 2D images (64×64 pixels) typically retrieved at the receiving end. The PSNR and SSIM values are given.

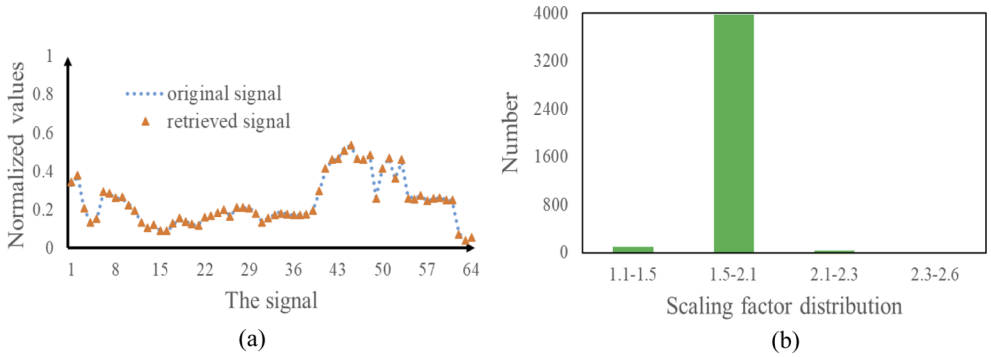

Fig. 12. (a) A comparison between pixel values along the 55th row of the retrieved image in Fig. 11(c) and those along the 55th row of original image, and (b) a scaling factor distribution (magnitude of the coefficients: 0.2×10^{-11}) corresponding to that in Fig. 11(c).

Optics EXPRESS

4. Conclusion

A new and robust method has been proposed for NLOS free-space optical data transmission through complex media, and high-fidelity free-space optical data transmission through turbid water around a corner has been realized. Optical experiments have been conducted to verify the proposed method using different turbid water conditions, different separation distances around the corner and different detection angles of single-pixel detector. Optical experimental results demonstrate that the proposed method possesses high feasibility and high robustness when there are turbid water and obstacles in the wave propagation path. In addition, different signals, e.g., analog signals and grayscale images, are widely tested by using the proposed method. The proposed approach can effectively overcome the challenges in conventional NLOS free-space optical data transmission methods, i.e., low-fidelity analog-signal retrieval through turbid water, low light detection, low mobility and high pointing errors.

Funding. Hong Kong Research Grants Council (C5011-19G); Shenzhen Science and Technology Innovation Commission (JCYJ20160531184426473); The Hong Kong Polytechnic University (G-R006, 4-R006, 1-W167, 1-W19E).

Disclosures. The authors declare no conflicts of interest.

Data availability. Data underlying the results presented in this paper are not publicly available at this time but may be obtained from the authors upon reasonable request.

References

1. T. D. Dickey, "Emerging ocean observations for interdisciplinary data assimilation systems," J. Mar. Syst. **40-41**, 5–48 (2003).
2. M. A. Khalighi and M. Uysal, "Survey on free space optical communication: a communication theory perspective," IEEE Commun. Surv. Tutorials **16**(4), 2231–2258 (2014).
3. Z. Zeng, S. Fu, H. Zhang, Y. Dong, and J. Cheng, "A survey of underwater optical wireless communications," IEEE Commun. Surv. Tutorials **19**(1), 204–238 (2017).
4. C.-C. Kao, Y.-S. Lin, G.-D. Wu, and C.-J. Huang, "A comprehensive study on the internet of underwater things: applications, challenges, and channel models," Sensors **17**(7), 1477 (2017).
5. B. Cochenour, L. J. Mullen, and A. E. Laux, "Characterization of the beam-spread function for underwater wireless optical communications links," IEEE J. Oceanic Eng. **33**(4), 513–521 (2008).
6. M. Chitre, S. Shahabudeen, and M. Stojanovic, "Underwater acoustic communications and networking: recent advances and future challenges," Mar. Technol. Soc. J. **42**(1), 103–116 (2008).
7. J. Wang, J. Y. Yang, I. M. Fazal, N. Ahmed, Y. Yan, H. Huang, Y. Ren, Y. Yue, S. Dolinar, M. Tur, and A. E. Willner, "Terabit free-space data transmission employing orbital angular momentum multiplexing," Nat. Photonics **6**(7), 488–496 (2012).
8. G. Gibson, J. Courtial, M. J. Padgett, M. Vasnetsov, V. Pas'ko, S. M. Barnett, and S. Franke-Arnold, "Free-space information transfer using light beams carrying orbital angular momentum," Opt. Express **12**(22), 5448–5456 (2004).
9. H. M. Oubei, C. Li, K. H. Park, T. K. Ng, M. S. Alouini, and B. S. Ooi, "2.3 Gbit/s underwater wireless optical communications using directly modulated 520 nm laser diode," Opt. Express **23**(16), 20743–20748 (2015).
10. K. Nakamura, I. Mizukoshi, and M. Hanawa, "Optical wireless transmission of 405 nm, 1.45 Gbit/s optical IM/DD-OFDM signals through a 4.8 m underwater channel," Opt. Express **23**(2), 1558–1566 (2015).
11. A. Trichili, M. A. Cox, B. S. Ooi, and M. S. Alouini, "Roadmap to free space optics," J. Opt. Soc. Am. B **37**(11), A184–A201 (2020).
12. C. C. Davis, I. I. Smolyaninov, and S. D. Milner, "Flexible optical wireless links and networks," IEEE Commun. Mag. **41**(3), 51–57 (2003).
13. S. Arnon and D. Kedar, "Non-line-of-sight underwater optical wireless communication network," J. Opt. Soc. Am. A **26**(3), 530–539 (2009).
14. X. Sun, W. Cai, O. Alkhazragi, E.-N. Ooi, H. He, A. Chaaban, C. Shen, H. M. Oubei, M. Z. M. Khan, T. K. Ng, M.-S. Alouini, and B. S. Ooi, "375-nm ultraviolet-laser based non-line-of-sight underwater optical communication," Opt. Express **26**(10), 12870–12877 (2018).
15. G. Chen, Z. Xu, and B. M. Sadler, "Experimental demonstration of ultraviolet pulse broadening in short-range non-line-of-sight communication channels," Opt. Express **18**(10), 10500–10509 (2010).
16. X. Liu, S. Yi, X. Zhou, Z. Fang, Z. J. Qiu, L. Hu, C. Cong, L. Zheng, R. Liu, and P. Tian, "34.5 m underwater optical wireless communication with 2.70 gbps data rate based on a green laser diode with nrz-ook modulation," Opt. Express **25**(22), 27937–27947 (2017).
17. A. P. Mosk, A. Lagendijk, G. Lerosey, and M. Fink, "Controlling waves in space and time for imaging and focusing in complex media," Nat. Photonics **6**(5), 283–292 (2012).
18. I. M. Vellekoop and A. P. Mosk, "Focusing coherent light through opaque strongly scattering media," Opt. Lett. **32**(16), 2309–2311 (2007).

Optics EXPRESS

19. I. M. Vellekoop, "Feedback-based wavefront shaping," Opt. Express **23**(9), 12189–12206 (2015).
20. J. Tang, R. N. Germain, and M. Cui, "Superpenetration optical microscopy by iterative multiphoton adaptive compensation technique," Proc. Natl. Acad. Sci. U.S.A. **109**(22), 8434–8439 (2012).
21. E. Tajahuerce, V. Durán, P. Clemente, E. Irles, F. Soldevila, P. Andrés, and J. Lancis, "Image transmission through dynamic scattering media by single-pixel photodetection," Opt. Express **22**(14), 16945–16955 (2014).
22. K. L. C. Seow, P. Török, and M. R. Foreman, "Single pixel polarimetric imaging through scattering media," arXiv preprint arXiv: 2006.03793, (2020).
23. K. Soltanlou and H. Latifi, "Three-dimensional imaging through scattering media using a single pixel detector," Appl. Opt. **58**(28), 7716–7726 (2019).
24. Y. Xiao, L. Zhou, and W. Chen, "Experimental demonstration of ghost-imaging-based authentication in scattering media," Opt. Express **27**(15), 20558–20566 (2019).
25. V. Durán, F. Soldevila, E. Irles, P. Clemente, E. Tajahuerce, P. Andrés, and J. Lancis, "Compressive imaging in scattering media," Opt. Express **23**(11), 14424–14433 (2015).
26. P. Udabage, R. Sharma, D. Murphy, I. Mckinnon, and R. Beckett, "Size distribution of reconstituted skim milk using field-flow fractionation," J. Micro. Sep. **9**(7), 557–563 (1997).
27. L. Wind and W. W. Szymanski, "Quantification of scattering corrections to the Beer-Lambert law for transmittance measurements in turbid media," Meas. Sci. Technol. **13**(3), 270–275 (2002).
28. R. Joshi, T. O'Connor, X. Shen, M. Wardlaw, and B. Javidi, "Optical 4D signal detection in turbid water by multi-dimensional integral imaging using spatially distributed and temporally encoded multiple light sources," Opt. Express **28**(7), 10477–10490 (2020).
29. S. Komatsu, A. Markman, and B. Javidi, "Optical sensing and detection in turbid water using multi-dimensional integral imaging," Opt. Lett. **43**(14), 3261–3264 (2018).
30. S. Tang, Y. Dong, and X. Zhang, "On path loss of NLOS underwater wireless optical communication links," in *Proceedings of IEEE Conference on Oceans*, IEEE Xplore, 1–3 (2013).
31. Y. Zuo, H. Xiao, J. Wu, Y. Li, and J. Lin, "A single-scatter path loss model for non-line-of-sight ultraviolet channels," Opt. Express **20**(9), 10359–10369 (2012).
32. M. Dehshiri, S. G Sabouri, and A. Khorsandi, "Structural similarity assessment of an optical coherence tomographic image enhanced using the wavelet transform technique," J. Opt. Soc. Am. A **38**(1), 1–9 (2021).
33. Y. Xiao, L. Zhou, and W. Chen, "Wavefront control through multi-layer scattering media using single-pixel detector for high-PSNR optical transmission," Opt. Lasers Eng. **139**, 106453 (2021).
34. Y. Xiao, L. Zhou, and W. Chen, "High-fidelity ghost diffraction and transmission in free space through scattering media," Appl. Phys. Lett. **118**(10), 104001 (2021).